Plasma Sources Science and Technology

PAPER

Temporal evolution of electron density in a low pressure pulsed two-frequency (60 MHz/2 MHz) capacitively coupled plasma discharge

To cite this article: N Sirse *et al* 2014 *Plasma Sources Sci. Technol.* **23** 065046

View the article online for updates and enhancements.

Related content

- Pulsed plasma etching for semiconductor manufacturing
  Demetre J Economou
- Control of electron energy distributions and plasma characteristics of dual frequency, pulsed capacitively coupled plasmas sustained in Ar and Ar/CF4/O2
  Sang-Heon Song and Mark J Kushner
- Radio-frequency capacitively coupled plasmas in hydrogen excited by tailored voltage waveforms: comparison of simulations with experiments
  P Diomede, D J Economou, T Lafleur et al.

Recent citations

- Electron density modulation in a pulsed dual-frequency (2/13.56 MHz) dual-antenna inductively coupled plasma discharge
  Nishant Sirse *et al*

This content was downloaded from IP address 115.145.196.110 on 12/12/2017 at 01:51

IOP Publishing Plasma Sources Science and Technology
Plasma Sources Sci. Technol. **23** (2014) 065046 (8pp) doi:10.1088/0963-0252/23/6/065046

Temporal evolution of electron density in a low pressure pulsed two-frequency (60 MHz/2 MHz) capacitively coupled plasma discharge

N Sirse[1], M H Jeon[2], G Y Yeom[2,3] and A R Ellingboe[1,2]

[1] Plasma Research Laboratory, School of Physical Sciences, Dublin City University, Dublin 9, Ireland
[2] Department of Advanced Materials Science and Engineering, Sungkyunkwan University, Suwon, Gyeonggi-do, 440–746, South Korea
[3] SKKU Advanced Institute of Nanotechnology (SAINT), Sungkyunkwan University, Suwon, Gyeunggi-do 440–746, South Korea

E-mail: nishant.sirse@dcu.ie

Received 26 June 2014, revised 8 September 2014
Accepted for publication 30 September 2014
Published 11 November 2014

Abstract

Time-resolved electron density, n_e, is measured in a low pressure pulsed two-frequency capacitively coupled plasma discharge sustained in Ar and in $Ar/CF_4/O_2$ (80 : 10 : 10) gas mixture using a floating resonance hairpin probe. The top electrode is powered by 60 MHz in pulse mode and the bottom electrode is powered by 2 MHz in continuous wave mode. The dependence of time-resolved n_e on the low frequency (LF) and high frequency (HF) power levels, operating gas pressure, pulse repetition frequency (PRF) and duty cycle are investigated. It is found that the steady state n_e in the long on-phase is greatly influenced by the HF power level and slightly affected by the LF power level in both Ar and $Ar/CF_4/O_2$ plasma. The decay time of n_e is slow (∼30–90 μs) in the case of Ar plasma and strongly depends on the LF power level, whereas in the case of $Ar/CF_4/O_2$ gas mixture it is very fast (∼15 μs) and marginally dependent on LF power level. In Ar plasma the steady state n_e is increasing with a rise in operating gas pressure, however, in $Ar/CF_4/O_2$ plasma it first increases with gas pressure reaching to the maximum (at 20 mTorr) value and then decreases. The pressure dependence of decay time constant mimics the pressure variation of steady state n_e. Furthermore, it is observed that the on-phase electron density is greatly affected by changing the PRF and duty cycle. This effect is more prominent in $Ar/CF_4/O_2$ plasma when compared to Ar discharge. In addition, n_e is observed to overshoot the steady state densities in the beginning of the on-phase in $Ar/CF_4/O_2$ gas mixture, but this effect is either small or absent in the case of Ar plasma.

Keywords: pulsed capacitive discharge, hairpin probe, electron density, time resolved

(Some figures may appear in colour only in the online journal)

1. Introduction

Capacitively coupled plasma (CCP) discharges operating in the low pressure regime (∼10^{-3}–1 Torr) are the industry standard tool for etching technologies and thin film deposition. For several decades capacitive discharges excited by single radio-frequency (13.56 MHz) have been used. It is well known that by increasing the driving frequency, higher plasma density and ion current can be achieved at a given sheath voltage [1]. This allows an enhanced plasma processing rate. However the independent control of ion energy and ion flux is extremely important for preventing charge damage, especially when high

 © 2014 IOP Publishing Ltd Printed in the UK

aspect ratio contacts (HARCs) are desired. To accomplish this, use of second frequency was proposed [2]. In this type of discharge the ion flux is mostly governed by the high frequency (HF) component, whereas the low frequency (LF) component is responsible for the change in ion energy. These voltage waveforms are applied either on the same electrode (DF-CCPs) or on the opposite electrodes (two-frequency CCPs). In recent decades several theoretical [3–5], experimental [6–8] and simulation [9–12] studies were published to understand the physics of multiple frequency CCPs and the effect of discharge conditions (electrode gap, LF and HF power levels, gas pressure etc) on the plasma parameters. One of the common conclusions drawn was that the effect of the multiple frequencies is coupled i.e. the lower frequency can also contribute to electron heating. Thus, it is not possible to have complete independent control of ion energy and ion flux even with the multiple frequency excitations.

A different way of controlling the ion flux and ion energy independently based on the electrical asymmetry effect (EAE) has recently been proposed and validated using both experiments and simulations [13, 14]. In the EAE an electrical asymmetry is produced in a symmetric CCP discharge by using a fundamental frequency and its harmonic with a variable phase shift between the voltage waveforms. The phase shift results in a dc self-bias which varies according to the phase angle and can be used to control the ion energy onto the substrate. Significantly stronger dc self-bias can be maintained by using multiple consecutive harmonics. This was originally proposed by Schulze *et al* [15] based on PIC simulations and later experimentally verified by Delattre *et al* [16] using a tailored voltage waveform. In this type of discharge, ion flux is controlled by changing the number of harmonics composed in a pulsed-type voltage waveform. The ion energy still remains constant and thus provides highly promising results in the photovoltaic processing applications [16].

Most of the experimental studies performed in multiple frequencies CCP discharges have been done in argon (Ar), however, in the industrial relevant processing environment electronegative gases such as CF_4, SF_6 etc are mostly used. Few experimental studies have been done on this type of gas mixtures. Karkari *et al* [6] measured n_e in a symmetric DF-CCP plasma processing tool containing $Ar/O_2/C_4F_8$ gas mixtures with a different combination of LF (2 MHz) and HF (27 MHz) power levels. Using phase resolved optical emission spectroscopy (PROES) Schulze *et al* [7] probed the electron dynamics and the power coupling mechanisms in the same discharge. They found that the separate control of plasma density and ion energy is rather complex. With cavity ring-down spectroscopy, fluorine negative ion densities were detected [17] in a 2 + 27 MHz dual frequency capacitive discharge in $Ar/CF_4/O_2$ and $Ar/C_4F_8/O_2$ mixtures. This was later [18] verified by measurements of density made by the combination of hairpin probe and ion flux probe. In another study done by Booth *et al* [8] the effect of LF power levels on n_e and ion flux was systematically investigated in Ar/O_2 and $Ar/O_2/C_4F_8$ gas mixtures in a 2/27 MHz DF-CCP. They found that the plasma density is significantly affected by the LF power level and attributed this to the enhanced plasma heating by DF excitations and the secondary electron beam ionization. Chen *et al* [19] performed measurements of electron temperature and electron energy distribution function (EEDFs) in a two-frequency CCP CF_4/O_2 based plasma etcher excited by 60 MHz source power and 13.56 MHz bias power using trace rare gas optical emission spectroscopy (TRG-OES). It was shown that the increase in the bias rf power resulted in higher electron temperature. A bi-Maxwellian EEDF with an enhanced high energy tail was observed at a pressure of less than 20 mTorr. More recently [20] an experimental investigation of steady state n_e and ion energy distribution (IED) was carried out in a DF (2/60 MHz) CCP discharge produced in Ar/CF_4 and $Ar/CF_4/O_2$ gas mixture. In this study a floating resonance hairpin probe and quadrupole mass spectrometer was used to investigate the effect of plasma controlling parameters (such as LF and HF power levels and gas pressure) on n_e and IED. It is observed that the n_e goes up rapidly to a maximum value with pressure and then decreases with further increase in gas pressure for several combinations of LF and HF power level.

Discharge pulsing is also an effective way to control the plasma chemistries. In pulsed plasma during the off-period the electron temperature can drop significantly while maintaining the adequate plasma density. Pulse plasma also offers higher production of chemically active species compared with a continuous discharge for the same average power [21]. It is an efficient way to produce negative ions in the plasmas. These negative ions are dominantly formed in the afterglow plasma where the electron temperature drops rapidly. It has been shown that the negative ion generation in the afterglow reduces the charge accumulation on the substrate during the plasma etching process [22]. Using emission-selected computerized tomography in a two-frequency CCP Ar/CF_4 plasma Ohmori *et al* [23] validated the formation of the negatively charged layer closest to the substrate when the powered electrode (100 MHz operating frequency) is pulsed (20 μs pulse period with 50% duty cycle). Pulsed plasma also maintains high etch selectivity compared to continuous wave (CW) plasma [24]. Using computer simulation, Song and Kushner [25] reported the effect of pulsing parameters on electron energy distribution function in a pulsed two-frequency CCP sustained in Ar and $Ar/CF_4/O_2$ mixture. They showed that the electron energy distribution function can be customized by varying the duty cycle and pulse repetition frequency (PRF). In an experimental study using an electron-emitting probe Mishra *et al* [26] measured the temporal evolution of the plasma potential in a pulsed two-frequency capacitive coupled Ar plasma. They found that the rf biasing of the substrate significantly affects the plasma potential. The effect was more prominent in the pulse off period and was reduced with an increase in gas pressure. Samara *et al* [27] investigated the effect of power modulation in a pulsed radio frequency capacitive discharge operated in Ar. In this study, electron density, electron temperature and light emission from the plasma was systematically measured with a tailored pulse waveform. They showed that the ignition phase and the afterglow decay processes can be controlled by modulating the applied pulse waveform. From the literature, it is evident that the multiple frequency CCP systems operated

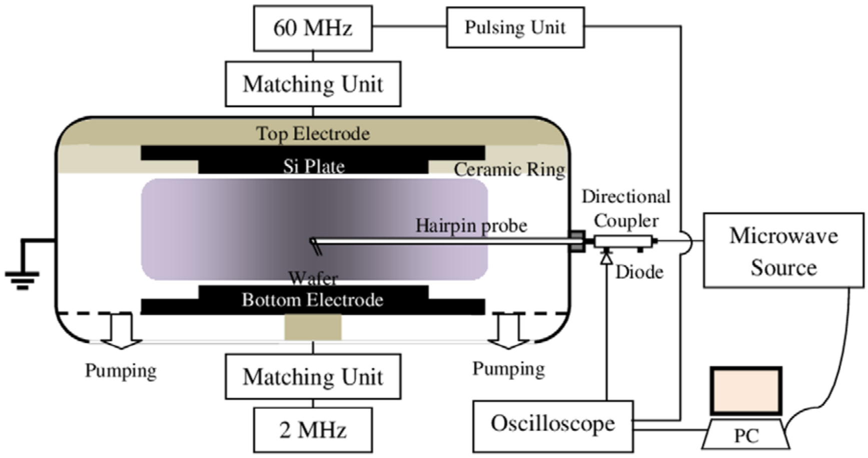

Figure 1. Schematic of the pulsed two-frequency CCP reactor used in this study along with the hairpin probe and the data acquisition system.

in pulse mode are an efficient way to achieve charge-free and highly selective plasma etching [23]. However the effect of pulsing on the plasma density evolution has not been studied in a two-frequency CCP discharge.

In this article we present an experimental study of temporal evolution of n_e in a pulsed two-frequency CCP (2/60 MHz) discharge. The temporal evolution of the plasma potential and electron temperature in Ar plasma was recently reported in this discharge [26]. Here we extend this study to investigate the $Ar/CF_4/O_2$ gas mixture. The effect of LF and HF power levels, gas pressure, PRF and duty cycle on the temporal evolution of n_e is reported. The experimental data are presented for both Ar and $Ar/CF_4/O_2$ gas mixture for comparison. It is observed that the steady state n_e is greatly affected by the HF power level and slightly affected by the LF power level in both Ar and $Ar/CF_4/O_2$ gas mixture. In Ar plasma the n_e decay time is very slow and greatly affected by the LF power level. Due to higher volumetric losses in $Ar/CF_4/O_2$ gas mixture the density decay time is very fast in comparison to the Ar plasma and depends marginally on the LF power level. There is an overshoot in the plasma density from steady state density observed in the beginning of the on-phase in $Ar/CF_4/O_2$ gas mixture; this overshoot is either absent or very low in the case of Ar plasma. The effect of gas pressure on plasma density decay is also studied. It is observed that the plasma density in the on-phase is highly influenced by the PRF and duty cycle. This observed effect is higher in the case of $Ar/CF_4/O_2$ gas mixture.

2. Experimental set-up and diagnostic technique

The schematic of the pulsed two-frequency CCP reactor under investigation [26] is shown in figure 1 along with the hairpin probe set-up. The discharge is produced in a cylindrical vessel made of anodized aluminum with internal diameter ~300 mm using two parallel-plate electrodes. The electrodes are 200 mm in diameter and separated by 40 mm. The top electrode is made of silicon incorporated with a showerhead to facilitate uniform flow of reactive species and further supported by an aluminum ring and a ceramic ring. The bottom electrode is made-up of anodized aluminum and cooled to the room temperature by a chiller. The top electrode is powered by a 60 MHz advanced energy ovation power generator via a matchbox. The output of the power generator is pulsed using a pulsing unit with an ability to change the pulse frequency and duty cycle. In the experiments the matching unit is tuned in CW mode to get minimum reflected power (<5 W). The bottom electrode is powered by a separate 2 MHz advanced energy ovation power generator and a matching unit with an incorporated blocking capacitor. The gas pressure in the chamber is regulated by a throttle valve above an EBARA turbo molecular pump (pumping speed ~3200 l s^{-1}) backed by a rotary pump.

Electron density is measured by using a microwave resonance hairpin probe. The principle behind the hairpin probe and the technique for measuring time resolved n_e, temporal resolution and the sensitivity of the hairpin probe for measuring the changes in n_e is very well described in the literature [28–31]. Briefly, in order to measure a time-resolved resonance frequency of the hairpin structure a single frequency output from a microwave generator is fed into the coupling loop via a directional coupler and a 50 Ω coaxial line. The reflected signal from the non 50 Ω (coupling loop) termination is measured using a Schottky diode and recorded on the oscilloscope. The oscilloscope is triggered by a suitable pulse waveform. If the hairpin structure is in resonance at any point of time during the oscilloscope collection period the reflected power shows a minimum at that point in time. Assuming that the electron density dynamic is repeated at each trigger pulse, in this case it is possible to tune the microwave source to the next higher frequency, which will allow the probe to resonate at a later time for increasing density. The process can be repeated to obtain a spectrum of probe resonance frequencies as a function of time, and then it is straightforward to obtain time-resolved n_e using $n_e(t) = \left(f_r^2(t) - f_0^2\right)/0.81$, where $fr(t)$ is the time varying resonance frequency in the plasma and f_0 is the vacuum resonance frequency. In this experiment the microwave generator and the oscilloscope are controlled by using a Labview^{TM} program developed at Dublin City University, Ireland. The frequency of the microwave generator is changed from 2.2-4 GHz in the step size of 10–15 MHz. This allows the lowest electron measurements

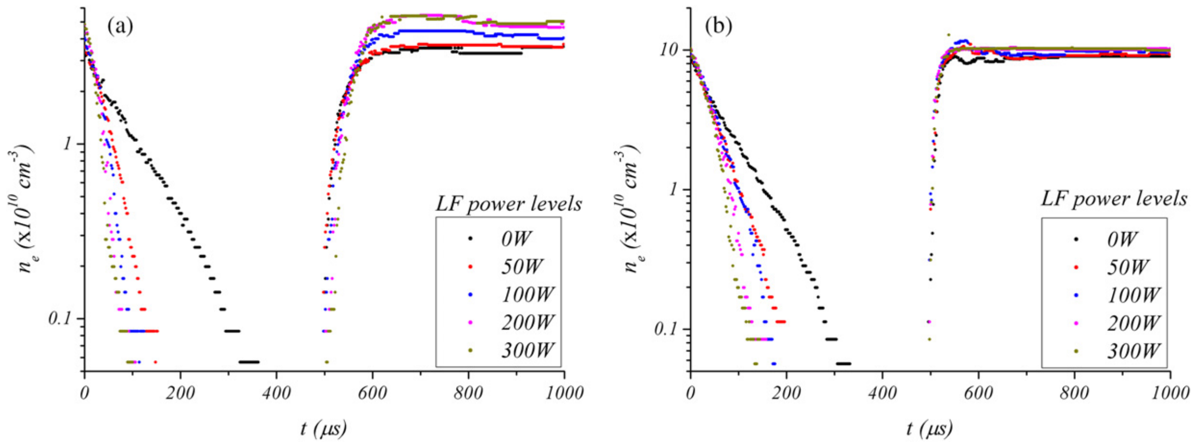

Figure 2. Temporal evolution of n_e measured in Ar plasma at different LF (2 MHz) power levels and 20 mTorr gas pressure for (*a*) 100 W and (*b*) 300 W 60 MHz peak power. Pulsing frequency is 1 kHz with 50% duty cycle.

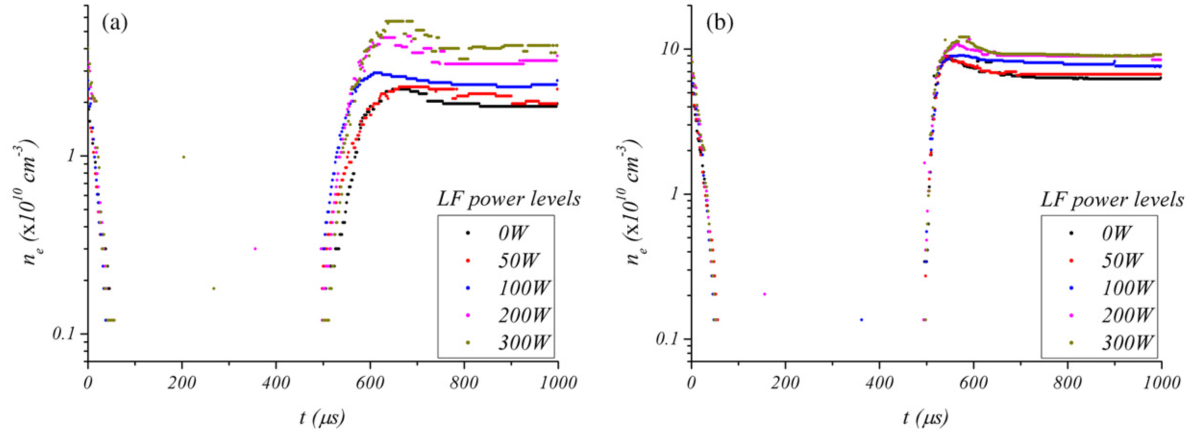

Figure 3. Temporal evolution of n_e measured in $Ar/CF_4/O_2$ plasma at different LF (2 MHz) power levels and 20 mTorr gas pressure for (*a*) 100 W and (*b*) 300 W 60 MHz peak power. Pulsing frequency is 1 kHz with 50% duty cycle.

from (0.6–0.9) $\times 10^9$ cm^{-3}. To increase signal-to-noise ratio the dc level at each frequency is first collected and then subtracted from the signal in plasma. The hairpin structure used in this study is ~30 mm in length, ~3 mm wide and made of 0.25 mm diameter tungsten wire. The measured vacuum resonance frequency of the probe is ~2.3 GHz.

3. Results and discussions

3.1. Effect of LF and HF power levels

Figures 2(*a*) and (*b*) shows the temporal evolution of n_e measured in Ar plasma as a function of LF power level for 100 W and 300 W HF power respectively. The probe is positioned at the centre of discharge and at a fixed vertical position of ~1.5 cm from the bottom electrode. In this experiment the pulsing frequency is set at 1 kHz with 50% duty cycle. The electron density data shown in each figure is starting from 0.5 $\times 10^9$ cm^{-3} since the lowest n_e measured by the probe is 0.6 $\times 10^9$ cm^{-3}. As observed the steady state n_e is affected by both LF and HF power levels. As illustrated in figure 2, the n_e becomes almost double i.e. increased from (4–6) $\times 10^{10}$ cm^{-3} to (9–12) $\times 10^{10}$ cm^{-3} with the rise in the 60 MHz peak power from 100 to 300 W, whereas, on increasing LF power level from 0 to 300 W the n_e increases by ~40% and 14% at 100 W and 300 W 60 MHz peak power respectively. This observed increase in n_e with a rise in LF and HF power level is due to the increase in power dissipation in the plasma volume. Increased power dissipation increases ionization in the plasma and therefore produces higher n_e. In addition the LF enhances stochastic heating in the multiple frequency capacitive discharges that causes the plasma density to increase with the rise in LF power level [4, 32]. Another possible heating mechanism by 2 MHz power level is the ionization caused by secondary electron beams [6, 8]. It is observed that the influence of low LF power level on steady state n_e is higher at low value of 60 MHz power level (100 W). This effect is mainly due to the increase in sheath width with decreasing 60 MHz power level.

In a different experimental run and under similar operating conditions n_e is measured in $Ar/CF_4/O_2$ (80 : 10 : 10 sccm) gas mixture. The results are shown in figures 3(*a*) and (*b*) for 100 W and 300 W 60 MHz peak power respectively. As shown in figure 3(*a*) the steady state n_e in $Ar/CF_4/O_2$ plasma ((1.89–4) $\times 10^{10}$ cm^{-3} @ 0–300 W LF power) is low compared to Ar plasma ((3.5–5) $\times 10^{10}$ cm^{-3} @ 0–300 W LF power). Similar results are found at 300 W in which a drop of 30% in the steady state n_e is observed in the $Ar/CF_4/O_2$ gas mixture when compared to Ar discharge. The decrease in the electron density on adding CF_4 and O_2 to Ar is attributed to increased electron losses in the plasma and power losses to the plasma chemistry. On addition of molecular gases (CF_4/O_2) electronically, vibrationally and rotationally excited states are produced that increase the collisional energy loss per electron–ion pair created in comparison to Ar discharge. This effect is dominant at low electron energy where the losses are mainly excitation losses [33]. Furthermore CF_4 and O_2 are electronegative gases and have a tendency to form negative ions through electron attachment process. Thus the low energy electrons are lost while the negative ions are produced in $Ar/CF_4/O_2$ plasma through dissociative attachment that contributes to the decrease in the electron density in $Ar/CF_4/O_2$ gas mixture. Similar to Ar discharge the steady state n_e is increasing with a rise in the LF and HF power levels.

As illustrated in figures 3(*a*) and (*b*) the n_e overshoots in the beginning of on-phase before reaching to the steady state density. This overshoot is either absent or very small in the case of Ar plasma. This behaviour is due to the increase in ionization rate coefficient in the beginning of the on-phase. In $Ar/CF_4/O_2$ gas mixture this effect is greater due to compensation in the volumetric electron losses [25]. Additionally the low dc conductivity caused by low electron density sets up a strong electric field in the beginning of the on-phase due to depletion of electrons that enhances the ionization and causes an overshoot in the electron density. This effect is similar to the drift-ambipolar heating mode effect as investigated by Schulze *et al* [34] for electronegative capacitive radio frequency plasmas. The overshoot in n_e from steady state density increases by nearly 20% on increasing HF power levels from 100 to 300 W with 0 W LF power. However the effect of 2 MHz power on electron density overshoot is non-monotonic i.e. it first decreases (up to 100 W) and then increases.

Focusing on the electron density transition over the course of one pulse period it is observed that the n_e increases during on-phase and decays during the off-phase. As shown in figures 2(*a*) and (*b*) the decay time of n_e in Ar is slow and strongly depends on the LF power level. The decay time constant as a function of LF power level is plotted in figure 4 for 100 W and 300 W HF peak power. As shown, the decay time constant is decreasing ($\sim$85 to $\sim$25 μs at 100 W HF power and from $\sim$70 to 40 μs at 300 W HF power level) with a rise in the LF power level from 0 to 300 W. In low pressure Ar plasma surface recombination is by-far the dominant loss mechanism and the decay rate is described by the Bohm flux to the surface which is linearly dependent on the density and the ion loss speed i.e. $dn/dt = nu_B$ where $u_B = \sqrt{kT_e}/M$, is the Bohm speed, k is the Boltzmann constant, T_e is the electron temperature and M is the positive ion mass. For constant T_e this equation describes an exponential decay in ion density with time, $n(t) = n_0\exp(-u_B t/2x)$ where x is the characteristic decay length (2 cm in our case), which agrees well with our measured electron decays in the HF off-phase, see figure 2. Consider first the temporal evolution in Ar plasma with no LF power, figure 2(*a*). When the HF power is turned off there is no heating of the electrons, they quickly cool and the Bohm speed decreases. The measured n_e shows an approximately linear decay with a characteristic time constant of $\sim$85 μs. Following from equations ($n(t)$ and u_B) this corresponds to an electron temperature of $\sim$0.1 eV. In contrast, when LF is not zero, the LF power maintains heating the electrons, but with much lower ionization efficiency such that the LF-only steady-state density is much lower. The decay rate is again governed by the ion loss speed, and the characteristic decay time of nearly 25 μs equates to an electron temperature of 1.5 eV, which is within a factor of two of the value predicted by a simple global-model particle-balance argument [35]. There is a slight decay-time dependence on LF power, with higher LF decaying faster (figure 4).

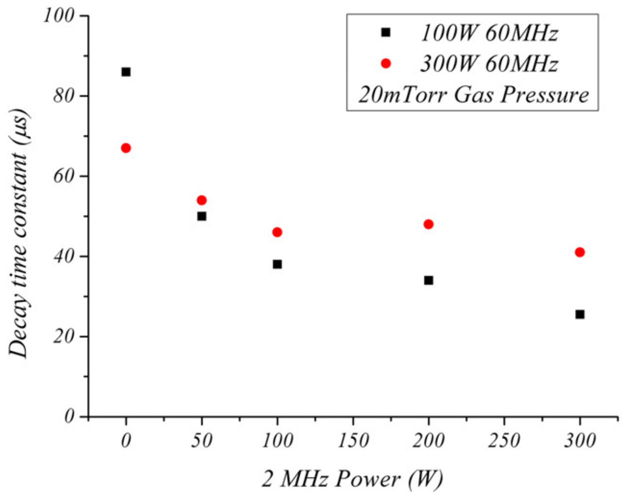

Figure 4. Decay time constant of n_e in Ar plasma versus LF power for 100 W and 300 W 60 MHz peak power. Pulsing frequency is 1 kHz with 50% duty cycle.

In contrast, in $Ar/CF_4/O_2$ gas mixtures (figure 3) the decay-rate is much faster ($\sim$15 μs) and has no discernible dependence on LF power. Fast decay of n_e in the case of $Ar/CF_4/O_2$ plasma was also observed in the recent simulation results [25]. This observed effect is attributed to the higher rate of volumetric electron losses in $Ar/CF_4/O_2$ plasma due to recombination and dissociative attachment. Electron temperature also decays at the faster rate in $Ar/CF_4/O_2$ plasma as compared to Ar plasma due to the higher collisional energy losses in the molecular component of the neutral gas [36]. This favours the negative ion formation in the afterglow plasma ($Ar/CF_4/O_2$) due to the electron attachment process and thus the electrons are lost quickly [37]. In contrast, in Ar plasma the volumetric losses such as dissociative recombination, three-particle recombination and radiative recombination are only relevant at high gas pressure or at the edge of the plasma [25]. The marginal dependence of density decay time constant on LF power level suggest that the volumetric losses are higher in $Ar/CF_4/O_2$ gas mixture in comparison to the wall losses.

3.2. Effect of gas pressure

Figure 5(*a*) shows the temporal evolution of n_e as a function of gas pressure in Ar plasma at 100 W LF power and 100 W HF

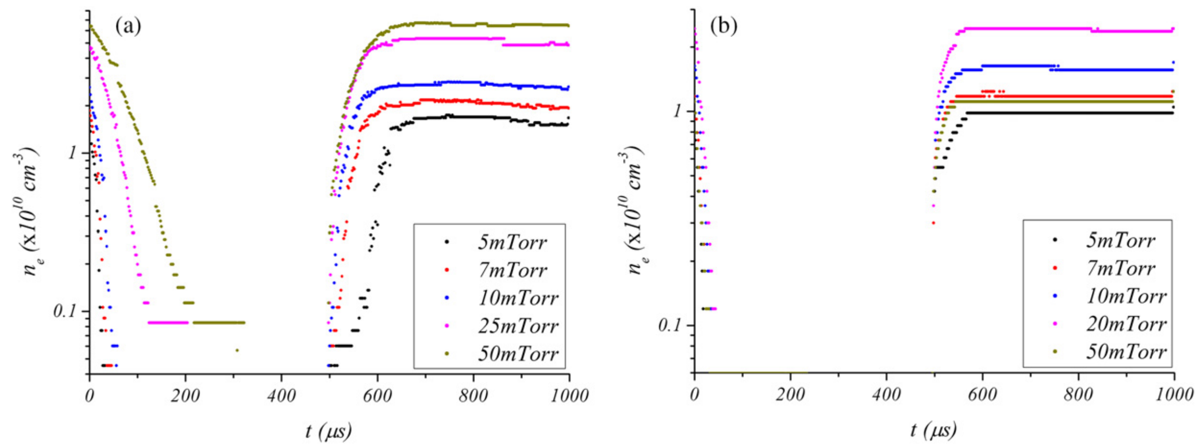

Figure 5. Temporal evolution of n_e in (*a*) Ar and (*b*) $Ar/CF_4/O_2$ plasma as a function of gas pressure. LF power level is fixed at 100 W. The 60 MHz peak power is 100 W with pulsing frequency and duty cycle of 1 kHz and 50% respectively.

power. The pulsing frequency is 1 kHz with 50% duty cycle. As shown in the figure the steady state n_e is increasing with the increase in gas pressure with a maximum of $6.5 \times 10^{10}\,cm^{-3}$ at 50 mTorr gas pressure. It is well known that low pressure CCP discharges are mostly sustained by the collisionless sheath heating mechanism [32]. In this type of heating mechanism electrons gain energy from the high-voltage oscillating sheath. This high-energy electron produces ionization in the bulk plasma, which further enhances with a rise in the gas pressure due to increase in the collisionality and thus produces high n_e. This result is consistent with the recent simulation results obtained in a low pressure Ar CCP discharge [38]. However, in $Ar/CF_4/O_2$ plasma it is observed that the steady state n_e increases with gas pressure in the range of 5 to 20 mTorr, peaking at the density of $2.5 \times 10^{10}\,cm^{-3}$, and then decreases with further increase in gas pressure. The initial increase in n_e with gas pressure is mainly due to increase in the ionization process, however, with further increase in gas pressure the volumetric electron losses such as recombination, detachment increases cause a decrease in n_e. This behaviour is well known in steady state electronegative plasmas [20].

As shown in figure 5(*a*) the n_e decay rate increases from 15 to 70 μs with increase in gas pressure from 5 to 50 mTorr. However, in $Ar/CF_4/O_2$ gas mixture the decay time constant mimics the trend of steady state n_e versus pressure i.e. it first increases with pressure and then decreases (figure 5(*b*)). It is observed that the decay time constant increases from $\sim$11 to 17 μs by changing pressure from 5 to 20 mTorr and then drops down to $\sim$10 μs at 50 mTorr gas pressure. In Ar plasma the slow decay of n_e with increasing gas pressure is due to a decrease in the electron temperature. According to the global model [36], in Ar plasma the n_e decay for a pulse power modulated low-pressure discharge is given by the expression: $n_e(t) = n_{emax}\,(1 + 2\nu_\infty\,(t - \alpha\tau))^{-1/2}$, where n_{emax} is the electron density in the beginning of off-phase, α is the duty cycle and τ is the pulse period. ν_∞ is the loss rate given by $\nu_\infty = \left(\frac{eT_{e\infty}}{M}\right)^{1/2}\frac{1}{l_{eff}}$ where $T_{e\infty}$ is the equilibrium electron temperature, e is electron charge, M is the mass of positive ion and l_{eff} is the effective length. With an increase in the gas pressure the electron temperature decreases (by 1–2 eV on increasing gas pressure from 20 to 40 mTorr) as observed in the previous experimental studies in the same setup and under similar operating conditions [26] and therefore the loss rate decreases according to the above expression. Due to decrease in the loss rate the plasma density decay time constant increases. A similar trend is observed in $Ar/CF_4/O_2$ gas mixture in the pressure range of 5 o 20 mTorr, however, a decrease in the plasma density decay time constant at 50 mTorr in $Ar/CF_4/O_2$ plasma is again due to the higher volumetric losses.

3.3. Effect of duty cycle and PRF

Time-resolved n_e measured versus duty cycle and for a fixed pulse frequency of 1 kHz at 20 mTorr gas pressure is shown in figures 6(*a*) and (*b*) for Ar and $Ar/CF_4/O_2$ plasma respectively. LF and HF power level is fixed at 200 W. As shown in the figures peak n_e in the plasma on-phase is decreasing with an increase in the duty cycle. The effect is prominent in $Ar/CF_4/O_2$ plasma in which a 40% drop in the n_e is observed (from $11.2 \times 10^{10}\,cm^{-3}$ at 10% duty cycle to $6.5 \times 10^{10}\,cm^{-3}$ at 90% duty cycle). Additionally, in $Ar/CF_4/O_2$ gas mixture the plasma density overshoot observed in n_e from the steady state density in the beginning of off-phase is diminishing with increasing duty cycle. This is in agreement with the recent simulation result [25] in which an extension in the tail of electron energy distribution function to the higher energy is observed with decrease in the duty cycle. This effect is mainly due to an increase in the reduced electric field strength (E/N: where E is electric field and N is gas number density) in the beginning of the on-phase, which causes an increase in the high temperature electrons through stochastic heating. E/N overshoot depends on the conductivity of the plasma at the beginning of the on-phase which is lower in the case of lower duty cycle due to loss of the electrons in the long off-phase for constant pulsing frequency.

The effect of PRF on time-resolved n_e is also studied and presented in figures 7 and 8 for Ar and $Ar/CF_4/O_2$ gas mixture respectively. LF and HF power levels are fixed at 200 W and the corresponding operating gas pressure is 20 mTorr. The duty cycle is kept constant at 50%. In Ar discharge at $t = 0\,\mu$s

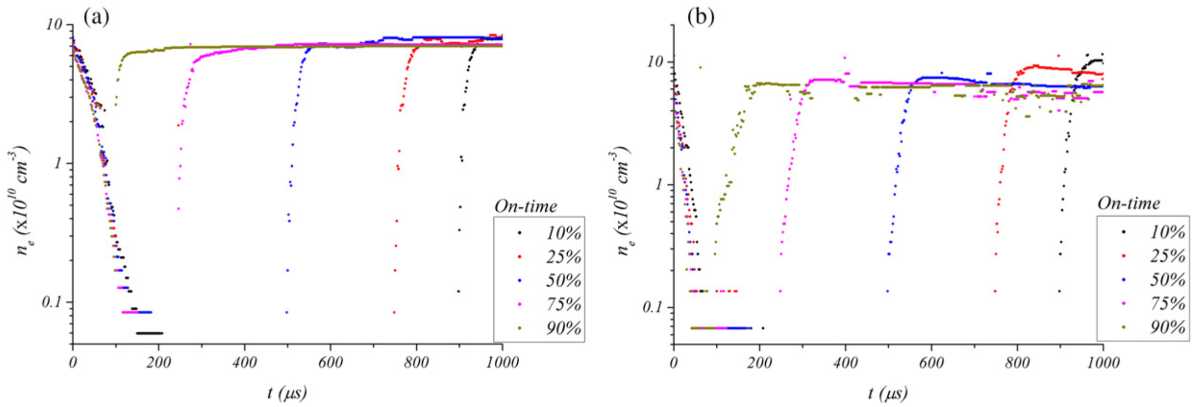

Figure 6. Effect of duty cycle on n_e (*a*) Ar (*b*) Ar/CF_4/O_2 plasma. LF and HF power levels are fixed at 200 W. 60 MHz pulsing frequency is 1 kHz and the operating gas pressure is 20 mTorr.

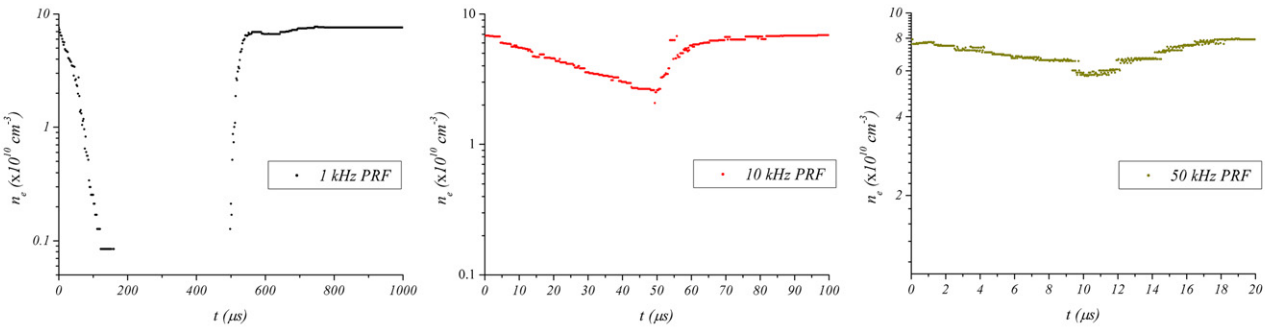

Figure 7. Effect of PRF on n_e in Ar plasma. LF and HF power levels are fixed at 200 W. The duty cycle is 50% and the operating gas pressure is 20 mTorr.

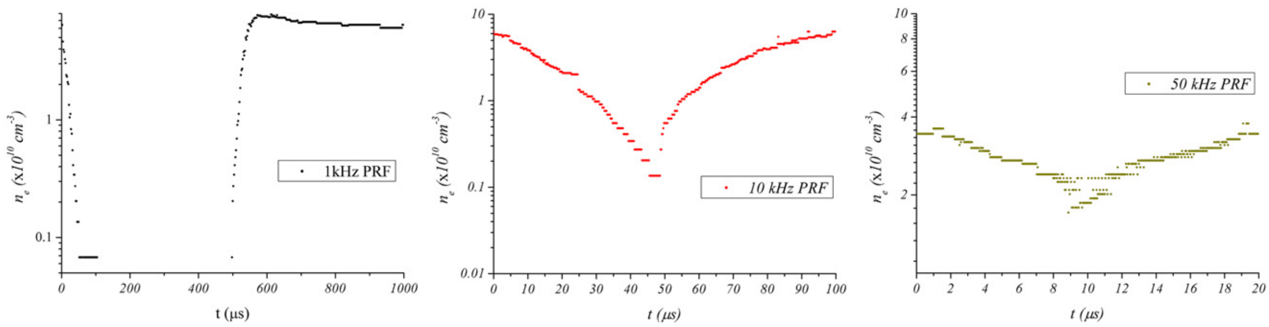

Figure 8. Effect of PRF on n_e in Ar/CF_4/O_2 plasma. LF and HF power levels are fixed at 200 W. The duty cycle is 50% and the operating gas pressure is 20 mTorr.

there is no significant change in the n_e observed with the rise in PRF from 1 kHz to 50 kHz. However, in case of Ar/CF_4/O_2 mixtures the steady state n_e are markedly different. At a frequency of 1 kHz an overshoot in the n_e with respect to steady state density is observed in the beginning of the on-phase which diminishes with a rise in the PRF. The maximum n_e measured during the overshoot phase is $\sim 8 \times 10^{10}\,cm^{-3}$ and reduced to $\sim 6.4 \times 10^{10}\,cm^{-3}$ in the steady state. The electron density decay time is smaller ($\sim$15 μs) compared to the interpulse period at 1 kHz pulse frequency (500 μs). As discussed in the previous paragraph the relative overshoot in the n_e depends on the rise in E/N which further depends on the plasma conductivity at the start of the on-phase. It is clear from the figure 8 that on increasing the PRF the n_e at the end of the off-phase is increasing and thus provides higher conductivity to the plasma on-phase.

4. Summary and conclusions

The temporal evolution of n_e is measured in a pulsed two-frequency CCP discharge sustained in Ar and Ar/CF_4/O_2 gas mixtures using a floating resonance hairpin probe. The effect of LF and HF power levels, gas pressure, duty cycle and pulse repetition frequency on the n_e is systematically investigated. It is observed that the steady state n_e increases with rise in LF and HF power levels in both Ar and Ar/CF_4/O_2 discharge. In Ar plasma the density decay time is slow and strongly depends on the LF power levels. On increasing the gas pressure the density decay time constant increases in Ar plasma, whereas, in the Ar/CF_4/O_2 gas mixture it first increases with operating gas pressure (11–17 μs at 5–20 mTorr gas pressure) and then decreases (10 μs at 50 mTorr). This is due to a decrease in the effective electron temperature measured previously in the same set-up and under similar discharge conditions using an emissive probe [26]. In Ar discharge the measured peak n_e in the plasma on-phase is decreasing with an increase in the duty cycle. However the effect of PRF on peak plasma density in the on-phase is negligible.

Similar to Ar discharge the steady state n_e is increasing in Ar/CF_4/O_2gas mixture with increased LF and HF power levels. However, in the Ar/CF_4/O_2gas mixture there is an overshoot in the n_e obtained in the beginning of the on-phase. This density overshoot is either absent or small in the case of Ar plasma. The decay time constant of n_e in Ar/CF_4/O_2 plasma is small compared to Ar plasma. This effect is attributed to the increase in the loss rate of n_e in Ar/CF_4/O_2 plasma. On increasing the duty cycle the peak n_e in the on-phase is decreasing and the n_e overshoot from steady state density is diminished. On the other hand with a rise in the pulse repetition frequency from 1 to 50 kHz there is a drop of ~50% n_e at $t = 0\,\mu$s observed in Ar/CF_4/O_2 discharge. From the measurements it is concluded that the plasma density decay time and its absolute value in the plasma on-phase are significantly affected by the LF power level. The effect is prominent at lower values of HF power level. The density decay time is greatly reduced by decreasing the operating gas pressure. Furthermore the choice of duty cycle and PRF can significantly alter the plasma density overshoot from the background density in the beginning of the on-phase.

Acknowledgments

This work was supported by the Korea Institute for the Advancement of Technology, Ministry of Knowledge Economy (L-2010-1438-000) Republic of Korea, Enterprise Ireland and the European Regional Development Fund (ERDF) under the National Strategic Reference Framework (NSRF) 2007–2013.

References

[1] Surendra M and Graves D B 1991 *Appl. Phys. Lett.* **59** 2091–3
[2] Goto H H, Lowe H D and Ohmi T 1992 *J. Vac. Sci. Technol.* A **10** 3048–54
[3] Robiche J, Boyle P C, Turner M M and Ellingboe A R 2003 *J. Phys. D: Appl. Phys.* **36** 1810–16
[4] Turner M M and Chabert P 2006 *Phys. Rev. Lett.* **96** 205001
[5] Kawamura E, Libermann M A and Lichtenberg A 2006 *J. Phys. Plasmas* **13** 063510
[6] Karkari S K and Ellingboe A R 2006 *Appl. Phys. Lett.* **88** 101501
[7] Schulze J, Gans T, O'Connell D, Czarnetzki U, Ellingboe A R and Turner M M 2007 *J. Phys. D: Appl. Phys.* **40** 7008–18
[8] Booth J P, Curley G, Maric D and Chabert P 2010 *Plasma Sources Sci. Technol.* **19** 015005
[9] Kim H C, Lee J K and Shon J W 2003 *Phys. Plasmas* **10** 4545–51
[10] Boyle P C, Ellingboe A R and Turner M M 2004 *J. Phys. D: Appl. Phys.* **37** 697–701
[11] Georgieva V and Bogaerts A 2005 *J. Appl. Phys.* **98** 023308
[12] Sharma S and Turner M M 2013 *J. Phys. D: Appl. Phys.* **46** 285203
[13] Schulze J, Schüngel E and Czarnetzki U 2009 *J. Phys. D: Appl. Phys.* **42** 092005
[14] Donko Z, Schulze J, Heil B G and Czarnetzki U 2009 *J. Phys. D: Appl. Phys.* **42** 025205
[15] Schulze J, Schüngel E, Donlo Z and Czarnetzki U 2011 *Plasma Sources Sci. Technol.* **20** 015017
[16] Delattre P A, Lafleur T, Johnson E V and Booth J P 2013 *J. Phys. D: Appl. Phys.* **46** 235201
[17] Booth J P, Corr C S, Curley G A, Jolly J and Guillon J 2006 *Appl. Phys. Lett.* **88** 151502
[18] Curley G A, Maric D, Booth J P, Corr C S, Chabert P and Guillon J 2007 *Plasma Sources Sci. Technol.* **16** S87–93
[19] Chen Z, Donnelly V M, Economou D J, Chen L, Funk M and Sundararajan R 2009 *J. Vac. Sci. Technol.* A **27** 1159–65
[20] Liu J, Liu Y X, Bi Z H, Gao F and Wang Y N 2014 *J. Appl. Phys.* **115** 013301
[21] Samukawa S and Furuoya S 1993 *Appl. Phys. Lett.* **63** 2044–6
[22] Samukawa S and Mieno T 1996 *Plasma Sources Sci. Technol.* **5** 132–8
[23] Ohmori T, Goto T and Makabe T 2004 *J. Phys. D: Appl. Phys.* **37** 2223–31
[24] Boswell R W and Henry D 1985 *Appl. Phys. Lett.* **47** 1095
[25] Song S H and Kushner M J 2012 *Plasma Sources Sci. Technol.* **21** 055028
[26] Mishra A, Jeon M H, Kim K N and Yeom G Y 2012 *Plasma Sources Sci. Technol.* **21** 055006
[27] Samara V, Bowden M D and Braithwaite N St J 2010 *J. Phys. D: Appl. Phys.* **43** 124017
[28] Karkari S K, Gaman C, Ellingboe A R, Swindells I and Bradley J W 2007 *Meas. Sci. Technol.* **18** 2649–56
[29] Conway J, Sirse N, Karkari S K and Turner M M 2010 *Plasma Sources Sci. Technol.* **19** 065002
[30] Bradley J W, Dodd R, You S-D, Sirse N and Karkari S K 2011 *J. Vac. Sci. Technol.* A **29** 031305
[31] Sirse N 2013 *PhD Thesis* Dublin City University, Ireland
[32] Turner M M 2009 *J. Phys. D: Appl. Phys.* **42** 194008
[33] Lee C and Libermann M A 1994 *J. Vac. Sci. Technol.* A **13** 368–80
[34] Schulze J, Derzsi A, Dittmann K, Hemke T, Meichsner and Donko Z 2011 *Phys. Rev. Lett.* **107** 275001
[35] Lieberman M A and Lichtenberg A J 1994 *Principles of Plasma Discharges and Materials Processing* (New York: Wiley)
[36] Lieberman M A and Ashida S 1996 *Plasma Sources Sci. Technol.* **5** 145–58
[37] Kono A, Haverlag M, Kroesen G M W and de Hoog F J 1991 *J. Appl. Phys.* **70** 2939
[38] Rauf S, Bera K and Collins K 2009 *Plasma Sources Sci. Technol.* **19** 015014